Supplement of

A seamless ensemble-based reconstruction of surface ocean pCO_2 and air–sea CO_2 fluxes over the global coastal and open oceans

Thi Tuyet Trang Chau et al.

Laboratoire des Sciences du Climat et de l'Environnement, LSCE/IPSL, CEA-CNRS-UVSQ, Université Paris-Saclay, F-91191 Gif-sur-Yvette, France

Correspondence: Thi Tuyet Trang Chau (trang.chau@lsce.ipsl.fr)

Table S1. Input fields for the CMEMS-LSCE-FFNN reconstruction of sea surface partial pressure of CO_2 (pCO_2) and air–sea CO_2 fluxes ($fgCO_2$) over the global ocean in 1985–2019.

Variables		Products	References
1	pCO_2 measurements	SOCATv2020, 1985-2019 (https://www.socat.info/)	Bakker et al. (2016)
2	Sea surface salinity (SSS)	CMEMS ARMOR3D L4, 1993-2019 (https://resources.marine.copernicus.eu/?option=com_csw&view=details&product_id=MULTIOBS_GLO_PHY_TSUV_3D_MYNRT_015_012)	Guinehut et al. (2012)
3	Sea surface height (SSH)		Mulet et al. (2012)
4	Sea surface temperature (SST)	CMEMS ARMOR3D L4, 1993-2019; OSTIA L4*, 1985-1992 (https://resources.marine.copernicus.eu/?option=com_csw&view=details&product_id=SST_GLO_SST_L4_REP_OBSERVATIONS_010_011)	Good et al. (2020)*
5	Mixed layer depth (MLD)	ECCO2, 1992-2019 (https://ecco.jpl.nasa.gov)	Menemenlis et al. (2008)
6	Chlorophyll (CHL)	GLOCOLOUR, 1998-2019 (https://www.globcolour.info/)	Maritorena et al. (2010)
7	CO_2 mole fraction (xCO_2)	CAMS CO_2 atmospheric inversion, 1985-2019 (https://atmosphere.copernicus.eu/)	Chevallier et al. (2005, 2010) Chevallier (2013)
8	pCO_2 climatology (pCO_2^{clim})	LDEO (https://www.ldeo.columbia.edu/res/pi/CO2/)	Takahashi et al. (2009)
9	6-hourly 10m winds	ERA5, 1985-2019 (https://www.ecmwf.int/en/forecasts/datasets/reanalysis-datasets/era5)	Hersbach et al. (2020)
10	Total pressure		
11	Sea ice fraction (f_{ice})	CMEMS OSTIA L4, 1985-2019, (https://resources.marine.copernicus.eu/?option=com_csw&view=details&product_id=SST_GLO_SST_L4_REP_OBSERVATIONS_010_011, https://resources.marine.copernicus.eu/?option=com_csw&view=details&product_id=SST_GLO_SST_L4_NRT_OBSERVATIONS_010_001)	Good et al. (2020)

**For some data unavailable before 1998, climatologies based on all available data were used as predictors. Exceptionally, predictors for SSH before 1993 are climatologies plus a linear trend in order to retain the overall response to the global warming. MLD before 1992 was taken as the average MLD between 1992 and 1997.

Table S2. Skill scores of the CMEMS-LSCE-FFNN reconstruction for different RECCAP regions. Validation between the reconstructed pCO_2 (μatm), $fgCO_2$ ($\mathrm{molC\,m^{-2}yr^{-1}}$), and the corresponding fields computed from SOCATv2020 data over the full period $1985-2019$. Statistical metrics include Root Mean Square Deviation (RMSD) and coefficient of determination (r^2).

	Regions	Number of observations		RMSD_{pCO_2}		$r^2_{pCO_2}$		RMSD_{fgCO_2}		$r^2_{fgCO_2}$	
		O	C	O	C	O	C	O	C	O	C
	Globe (G)	270228	31221	17.87	35.86	0.78	0.70	0.93	1.91	0.79	0.64
1	Arctic (Ar)	1170	449	33.01	30.65	0.61	0.44	1.11	0.93	0.70	0.77
2	Subpolar Atlantic (SpA)	24433	12249	23.68	30.35	0.76	0.79	1.35	1.66	0.69	0.75
3	Subpolar Pacific (SpP)	10840	3596	29.08	54.69	0.64	0.57	1.80	2.70	0.66	0.54
4	Subtropical Atlantic (StA)	50113	5205	15.24	34.74	0.76	0.51	0.77	2.39	0.77	0.37
5	Subtropical Pacific (StP)	67950	853	17.15	47.29	0.78	0.45	0.81	2.08	0.84	0.48
6	Equatorial Atlantic (EA)	11574	469	14.11	36.03	0.69	0.25	0.53	1.14	0.64	0.36
7	Equatorial Pacific (EP)	45590	221	16.68	27.17	0.80	0.41	0.57	0.84	0.81	0.38
8	South Atlantic (SA)	4577	562	14.09	37.98	0.77	0.46	0.71	2.00	0.78	0.42
9	South Pacific (SP)	17074	1181	11.50	14.38	0.76	0.60	0.56	0.71	0.79	0.62
10	Indian Ocean (IO)	7792	588	14.60	18.37	0.80	0.65	1.02	0.91	0.78	0.68
11	Southern Ocean (SO)	29115	5848	19.18	35.73	0.62	0.65	1.24	1.64	0.53	0.64

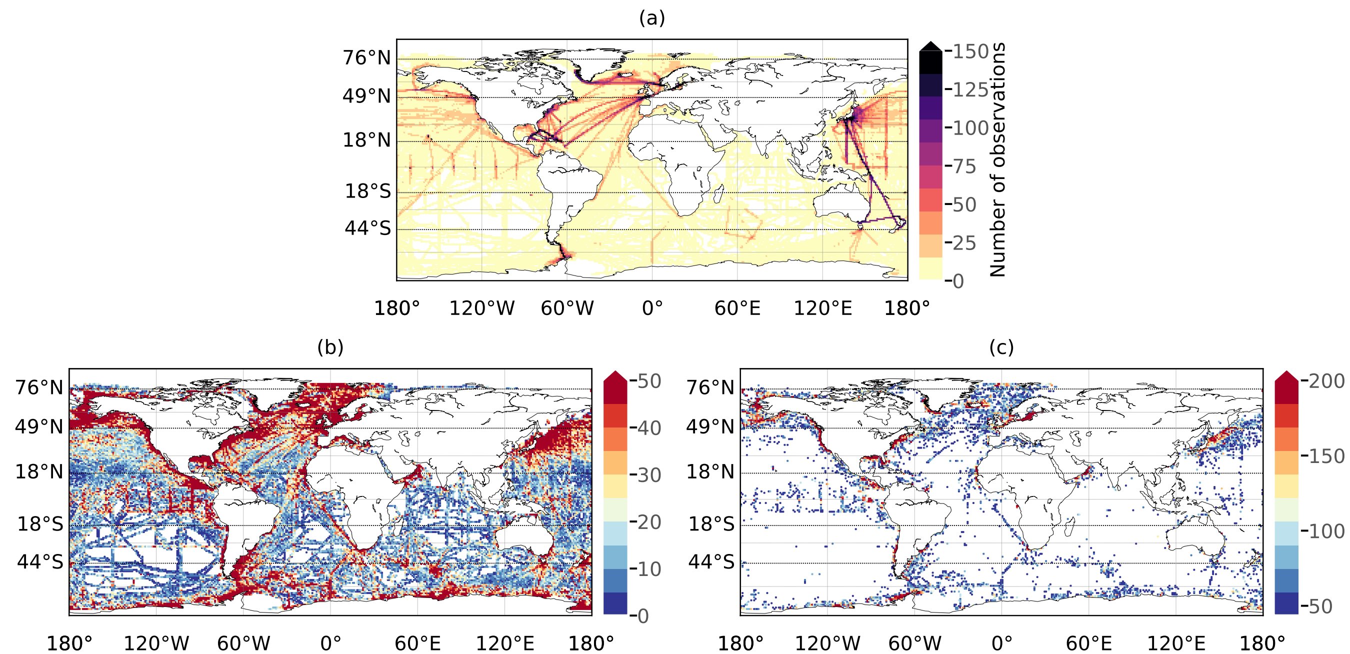

Figure S1. (a) Spatial distribution of monthly gridded SOCATv2020 data and (b,c) maximum spatial variability of SOCAT $p\mathrm{CO}_2$ individuals (μatm), i.e. $p\mathrm{CO}_{2,SOCAT}^{\max} - p\mathrm{CO}_{2,SOCAT}^{\min}$, measured within a $1^\circ \times 1^\circ$ box. Figure S1c shows the distribution of the spatial variability larger than the 80%-quantile.

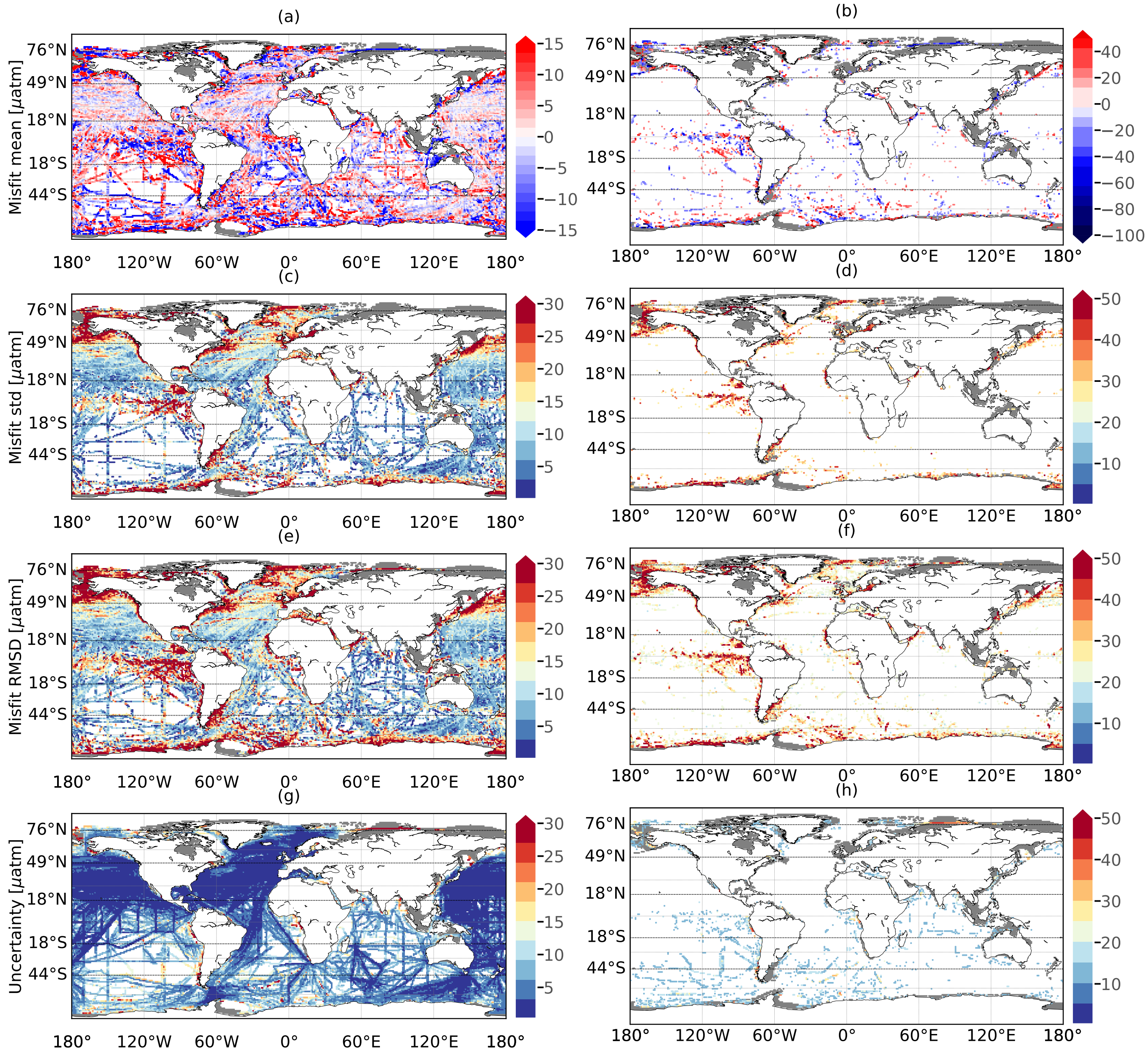

Figure S2. Temporal mean (a,b), standard deviation (c,d), and RMSD (e,f) of model-minus-observation misfits between the reconstructed $p\mathrm{CO}_2$ and SOCAT data; and model uncertainty (g,h), i.e. ensemble standard deviation of temporal mean estimates at SOCAT observation location. The right column plots show statistics falling out of the 90% quantile range for (b), or larger than the 90%-quantile for (d,f,h).

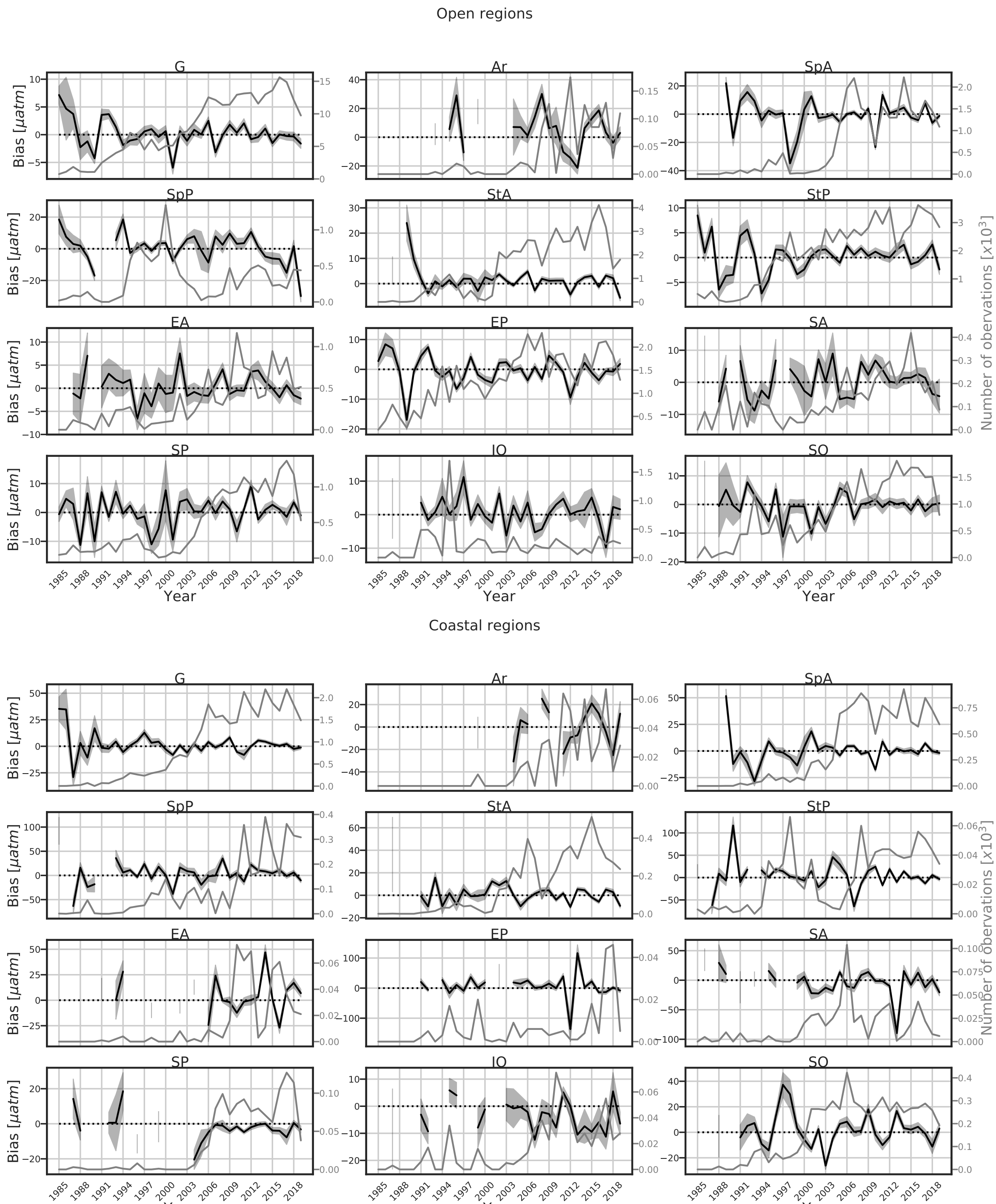

Figure S3. Timeseries of the yearly mean bias between the reconstructed $p\mathrm{CO}_2$ data and SOCATv2020 data over the open ocean and coastal area (black curve) and of the total number of observations used in the FFNN model construction (light grey curve). The grey area represents the 1σ-envelop of the errors derived from the 100-member ensemble.

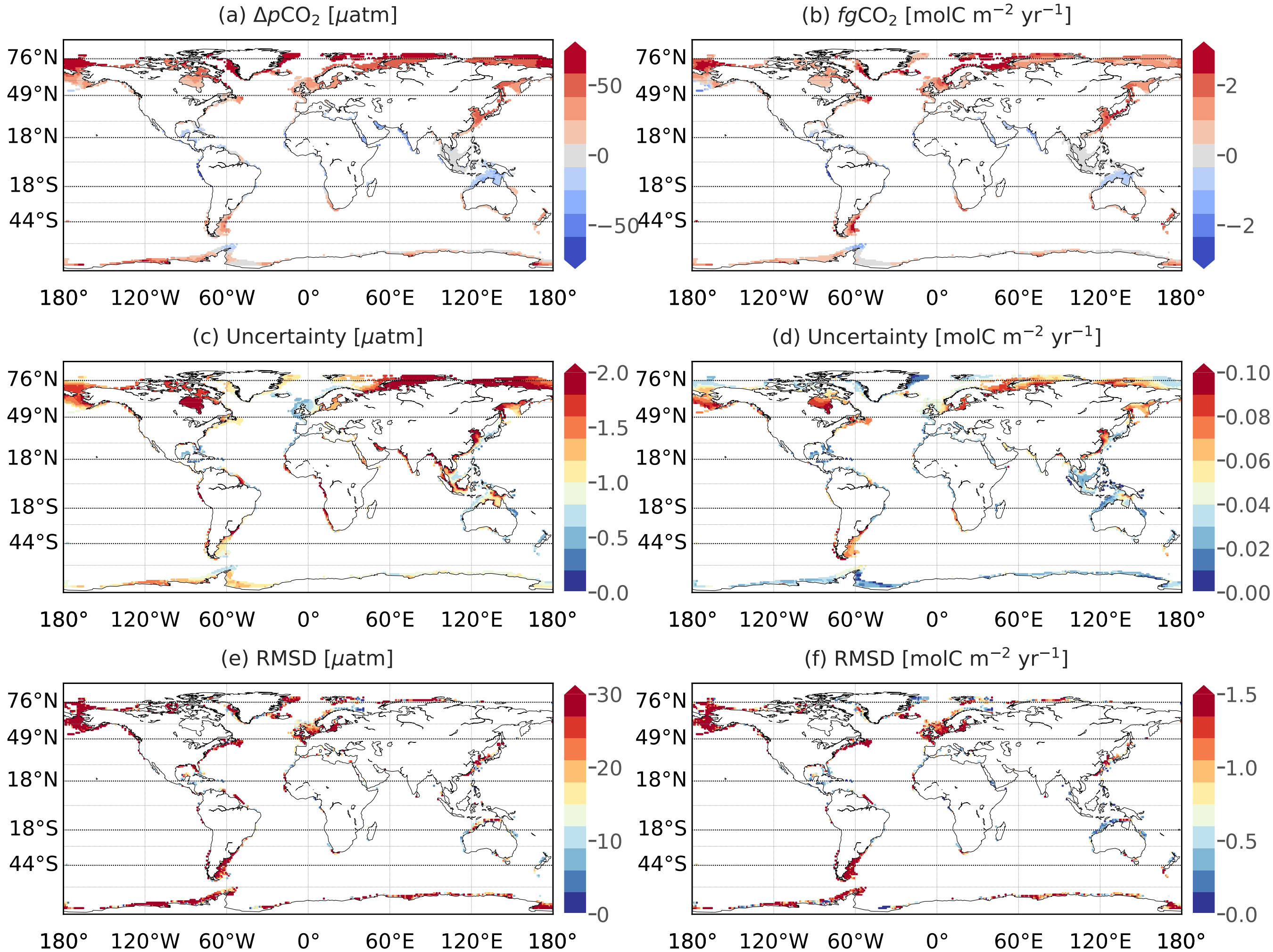

Figure S4. Climatological mean (top) and uncertainty (middle) of air-sea pCO_2 difference (a, c) and of CO_2 fluxes (b, d) over the coastal ocean for 1985-2019. Uncertainty is computed as standard deviation of the 100-member CMEMS-LSCE-FFNN model outputs of sea surface pCO_2 and air-sea CO_2 fluxes. The bottom plots (e, f) show RMSDs between the SOCAT data (or data-based estimates of fluxes for (f)) and the mean CMEMS-LSCE-FFNN model outputs.

References

Bakker, D. C. E., Pfeil, B., Landa, C. S., Metzl, N., O'Brien, K. M., Olsen, A., Smith, K., Cosca, C., Harasawa, S., Jones, S. D., Nakaoka, S., Nojiri, Y., Schuster, U., Steinhoff, T., Sweeney, C., Takahashi, T., Tilbrook, B., Wada, C., Wanninkhof, R., Alin, S. R., Balestrini, C. F., Barbero, L., Bates, N. R., Bianchi, A. A., Bonou, F., Boutin, J., Bozec, Y., Burger, E. F., Cai, W.-J., Castle, R. D., Chen, L., Chierici, M., Currie, K., Evans, W., Featherstone, C., Feely, R. A., Fransson, A., Goyet, C., Greenwood, N., Gregor, L., Hankin, S., Hardman-Mountford, N. J., Harlay, J., Hauck, J., Hoppema, M., Humphreys, M. P., Hunt, C. W., Huss, B., Ibánhez, J. S. P., Johannessen, T., Keeling, R., Kitidis, V., Körtzinger, A., Kozyr, A., Krasakopoulou, E., Kuwata, A., Landschützer, P., Lauvset, S. K., Lefèvre, N., Lo Monaco, C., Manke, A., Mathis, J. T., Merlivat, L., Millero, F. J., Monteiro, P. M. S., Munro, D. R., Murata, A., Newberger, T., Omar, A. M., Ono, T., Paterson, K., Pearce, D., Pierrot, D., Robbins, L. L., Saito, S., Salisbury, J., Schlitzer, R., Schneider, B., Schweitzer, R., Sieger, R., Skjelvan, I., Sullivan, K. F., Sutherland, S. C., Sutton, A. J., Tadokoro, K., Telszewski, M., Tuma, M., van Heuven, S. M. A. C., Vandemark, D., Ward, B., Watson, A. J., and Xu, S.: A multi-decade record of high-quality $f\mathrm{CO_2}$ data in version 3 of the Surface Ocean CO_2 Atlas (SOCAT), Earth Syst. Sci. Data, 8, 383–413, https://doi.org/10.5194/essd-8-383-2016, 2016.

Chevallier, F.: On the parallelization of atmospheric inversions of CO_2 surface fluxes within a variational framework, Geosci. Model Dev., 6, 783–790, https://doi.org/10.5194/gmd-6-783-2013, 2013.

Chevallier, F., Fisher, M., Peylin, P., Serrar, S., Bousquet, P., Bréon, F.-M., Chédin, A., and Ciais, P.: Inferring CO_2 sources and sinks from satellite observations: Method and application to TOVS data, J. Geophys. Res. Atmos., 110, https://doi.org/https://doi.org/10.1029/2005JD006390, 2005.

Chevallier, F., Ciais, P., Conway, T. J., Aalto, T., Anderson, B. E., Bousquet, P., Brunke, E. G., Ciattaglia, L., Esaki, Y., Fröhlich, M., Gomez, A., Gomez-Pelaez, A. J., Haszpra, L., Krummel, P. B., Langenfelds, R. L., Leuenberger, M., Machida, T., Maignan, F., Matsueda, H., Morguí, J. A., Mukai, H., Nakazawa, T., Peylin, P., Ramonet, M., Rivier, L., Sawa, Y., Schmidt, M., Steele, L. P., Vay, S. A., Vermeulen, A. T., Wofsy, S., and Worthy, D.: CO_2 surface fluxes at grid point scale estimated from a global 21 year reanalysis of atmospheric measurements, J. Geophys. Res. Atmos., 115, https://doi.org/https://doi.org/10.1029/2010JD013887, 2010.

Good, S., Fiedler, E., Mao, C., Martin, M. J., Maycock, A., Reid, R., Roberts-Jones, J., Searle, T., Waters, J., While, J., and Worsfold, M.: The current configuration of the OSTIA system for Operational Production of Foundation Sea Surface Temperature and Ice Concentration Analyses, Remote Sens., 12, https://www.mdpi.com/2072-4292/12/4/720, 2020.

Guinehut, S., Dhomps, A.-L., Larnicol, G., and Le Traon, P.-Y.: High resolution 3-D temperature and salinity fields derived from in situ and satellite observations, Ocean Sci., 8, 845–857, https://doi.org/10.5194/os-8-845-2012, 2012.

Hersbach, H., Bell, B., Berrisford, P., Hirahara, S., Horányi, A., Muñoz-Sabater, J., Nicolas, J., Peubey, C., Radu, R., Schepers, D., Simmons, A., Soci, C., Abdalla, S., Abellan, X., Balsamo, G., Bechtold, P., Biavati, G., Bidlot, J., Bonavita, M., De Chiara, G., Dahlgren, P., Dee, D., Diamantakis, M., Dragani, R., Flemming, J., Forbes, R., Fuentes, M., Geer, A., Haimberger, L., Healy, S., Hogan, R. J., Hólm, E., Janisková, M., Keeley, S., Laloyaux, P., Lopez, P., Lupu, C., Radnoti, G., de Rosnay, P., Rozum, I., Vamborg, F., Villaume, S., and Thépaut, J.-N.: The ERA5 global reanalysis, Q. J. R. Meteorol. Soc., 146, 1999–2049, https://doi.org/https://doi.org/10.1002/qj.3803, 2020.

Maritorena, S., d'Andon, O. H. F., Mangin, A., and Siegel, D. A.: Merged satellite ocean color data products using a bio-optical model: Characteristics, benefits and issues, Remote Sens. Environ., 114, 1791–1804, https://doi.org/https://doi.org/10.1016/j.rse.2010.04.002, 2010.

Menemenlis, D., Campin, J., Heimbach, P., Hill, C., Lee, T., Nguyen, A., Schodlok, M., and Zhang, H.: ECCO2: High resolution global ocean and sea ice data synthesis, OS31C-1292, 2008.

Mulet, S., Rio, M.-H., Mignot, A., Guinehut, S., and Morrow, R.: A new estimate of the global 3D geostrophic ocean circulation based on satellite data and in-situ measurements, Deep Sea Res. 2 Top. Stud. Oceanogr., 77-80, 70–81, https://doi.org/https://doi.org/10.1016/j.dsr2.2012.04.012, 2012.

Takahashi, T., Sutherland, S. C., Wanninkhof, R., Sweeney, C., Feely, R. A., Chipman, D. W., Hales, B., Friederich, G., Chavez, F., Sabine, C., Watson, A., Bakker, D. C., Schuster, U., Metzl, N., Yoshikawa-Inoue, H., Ishii, M., Midorikawa, T., Nojiri, Y., Körtzinger, A., Steinhoff, T., Hoppema, M., Olafsson, J., Arnarson, T. S., Tilbrook, B., Johannessen, T., Olsen, A., Bellerby, R., Wong, C., Delille, B., Bates, N., and de Baar, H. J.: Climatological mean and decadal change in surface ocean $p\mathrm{CO_2}$, and net sea–air $\mathrm{CO_2}$ flux over the global oceans, Deep Sea Res. 2 Top. Stud. Oceanogr., 56, 554–577, https://doi.org/https://doi.org/10.1016/j.dsr2.2008.12.009, 2009.